Evidence for primordial water in Earth's deep mantle

8 authors, including:

L. J. Hallis
University of Glasgow
47 PUBLICATIONS **250** CITATIONS

SEE PROFILE

Sæmundur Ari Halldórsson
University of Iceland
26 PUBLICATIONS **268** CITATIONS

SEE PROFILE

David R. Hilton
University of California, San Diego
271 PUBLICATIONS **6,096** CITATIONS

SEE PROFILE

M. J. Mottl
University of Hawai'i System
485 PUBLICATIONS **6,650** CITATIONS

SEE PROFILE

Some of the authors of this publication are also working on these related projects:

Stardust-NExT View project

Hydrogeochemical and Isotopic Investigation of Geothermal Systems of North Eastern Anatolia View project

12. A. Fleischer *et al.*, *Phys. Rev. Lett.* **107**, 113003 (2011).
13. F. Calegari *et al.*, *Science* **346**, 336–339 (2014).
14. O. Smirnova *et al.*, *Nature* **460**, 972–977 (2009).
15. Y. Mairesse *et al.*, *Phys. Rev. Lett.* **104**, 213601 (2010).
16. S. Haessler *et al.*, *Nat. Phys.* **6**, 200–206 (2010).
17. H. Niikura *et al.*, *Nature* **421**, 826–829 (2003).
18. M. Allan, E. Kloster-Jensen, J. P. Maier, *J. Chem. Soc. Faraday Trans. II* **73**, 1406–1416 (1977).
19. R. S. Mulliken, *J. Chem. Phys.* **7**, 20 (1939).
20. H. Stapelfeldt, T. Seideman, *Rev. Mod. Phys.* **75**, 543–557 (2003).
21. M. Lein, *Phys. Rev. Lett.* **94**, 053004 (2005).
22. S. Baker *et al.*, *Science* **312**, 424–427 (2006).
23. H. J. Wörner, J. B. Bertrand, P. Hockett, P. B. Corkum, D. M. Villeneuve, *Phys. Rev. Lett.* **104**, 233904 (2010).
24. R. Torres *et al.*, *Phys. Rev. A* **81**, 051802 (2010).
25. C. Vozzi *et al.*, *Nat. Phys.* **7**, 822–826 (2011).
26. S. De *et al.*, *Phys. Rev. Lett.* **103**, 153002 (2009).
27. X. Zhou *et al.*, *Phys. Rev. Lett.* **100**, 073902 (2008).
28. A.-T. Le, R. R. Lucchese, S. Tonzani, T. Morishita, C. D. Lin, *Phys. Rev. A* **80**, 013401 (2009).
29. M. Lewenstein, P. Balcou, M. Y. Ivanov, A. L'Huillier, P. B. Corkum, *Phys. Rev. A* **49**, 2117–2132 (1994).
30. M. V. Frolov, N. L. Manakov, T. S. Sarantseva, A. F. Starace, *J. Phys. B* **42**, 035601 (2009).
31. D. Shafir *et al.*, *Nature* **485**, 343–346 (2012).
32. E. F. Penka, E. Couture-Bienvenue, A. D. Bandrauk, *Phys. Rev. A* **89**, 023414 (2014).
33. O. I. Tolstikhin, T. Morishita, L. B. Madsen, *Phys. Rev. A* **84**, 053423 (2011).
34. A. Wirth *et al.*, *Science* **334**, 195–200 (2011).

GEOCHEMISTRY

Evidence for primordial water in Earth's deep mantle

Lydia J. Hallis,[1,2]*† Gary R. Huss,[1,2] Kazuhide Nagashima,[2] G. Jeffrey Taylor,[1,2] Sæmundur A. Halldórsson,[3]‡ David R. Hilton,[3] Michael J. Mottl,[4] Karen J. Meech[1,5]

The hydrogen-isotope [deuterium/hydrogen (D/H)] ratio of Earth can be used to constrain the origin of its water. However, the most accessible reservoir, Earth's oceans, may no longer represent the original (primordial) D/H ratio, owing to changes caused by water cycling between the surface and the interior. Thus, a reservoir completely isolated from surface processes is required to define Earth's original D/H signature. Here we present data for Baffin Island and Icelandic lavas, which suggest that the deep mantle has a low D/H ratio (δD more negative than −218 per mil). Such strongly negative values indicate the existence of a component within Earth's interior that inherited its D/H ratio directly from the protosolar nebula.

Establishing Earth's initial D/H ratio is important for understanding the origin of our planet's water, as well as the dynamical processes that operated during planet formation in the solar system. However, evolution of this ratio occurs over time as a result of surface and mantle processing. Collisions with hydrogen-bearing planetesimals or cometary material after Earth's accretion should have altered the D/H ratio of the planet's surface and upper mantle (*1*). In addition, experimentally based chemical models suggest an increase in the atmospheric D/H value by a factor of 2 to 9 since Earth's formation (*2*). Preferential loss of the lighter hydrogen isotope from the upper atmosphere causes this increase, driven by thermal atmospheric escape or plasma interactions with the atmosphere. As atmospheric D/H is linked with that of ocean water and sediments, the D/H ratio of the mantle also increases with time via subduction and convective mixing. Only areas of the deep Earth that have not participated in this mixing process are likely to preserve Earth's initial D/H ratio.

Studies of the trace-element, radiogenic-isotope, and noble gas isotope characteristics of mid-ocean ridge basalts (MORBs) and ocean-island basalts (OIBs) reveal the existence of domains within Earth's mantle that have experienced distinct evolutionary histories (*3*, *4*). Although alternative theories exist [e.g., (*5*)], most studies suggest that high $^3He/^4He$ ratios in some OIBs indicate the existence of relatively undegassed regions in the deep mantle compared to the upper mantle, which retain a greater proportion of their primordial He (*6*, *7*). Helium-isotope ($^3He/^4He$) ratios more than 30 times the present-day ratio of Earth's atmosphere ($R_A = 1.38 \times 10^{-6}$) (*8*) can be found in volcanic rocks from oceanic islands, including Iceland and Hawaii (*9–12*). Early Tertiary (60-million-year-old) lavas from Baffin Island and west Greenland, which represent volcanic rocks from the proto/early Iceland mantle plume, contain the highest recorded terrestrial $^3He/^4He$ ratios of up to 50 R_A (*6*, *7*). These lavas also have Pb and Nd isotopic ratios consistent with primordial mantle ages [4.45 to 4.55 billion years (Ga)] (*13*), indicating the persistence of an ancient, isolated reservoir in the mantle. The undegassed and primitive nature (*14*) of this reservoir means that it could preserve Earth's initial D/H ratio. This study targets mineral-hosted melt inclusions in these rocks in search of this primordial signal.

A range of D/H ratios are found on Earth. We compare the ratio of deuterium (^2H or D) to hydrogen (^1H) relative to Vienna Standard Mean Ocean Water (VSMOW, D/H = 1.5576 × 10^{-4}) using δD = {[(D/H)$_{unknown}$/(D/H)$_{VSMOW}$] − 1} × 1000, in units of parts per thousand [per mil (‰)]. The hydrological cycle fractionates hydrogen, creating glacial ice [standard Greenland Ice Sheet Precipitation δD = −190‰ (*15*)], ocean water (VSMOW δD = 0‰), and fresh water [δD = 0 to −300‰ (*16*)] reservoirs. Subduction provides a means to mix water back into the mantle, producing a variation in δD from −126 to +46‰ from slab dehydration and sediment recycling (*17*, *18*). The MORB source appears to be better mixed, with a uniform δD of −60 ± 5‰ (*19*).

We measured the D/H ratios of olivine-hosted glassy melt inclusions in two depleted picrite samples (basaltic rocks with abundant Mg-rich olivine) from Padloping Island, northwest Baffin Island (*20*), and in three picrite samples from Iceland's western and northern rift zones (*9–11*). The high forsterite (Fo) contents of these olivines (Fo$_{87-91}$) suggest crystallization from primitive melts (*21*). We monitored possible contamination from crustal materials, or meteoric water due to weathering, by measuring the oxygen-isotope ratios of the samples (*21*). One Icelandic sample shows slightly raised δ^{18}O, indicative of crustal contamination. All other samples fall within the range expected for uncontaminated mantle-derived samples.

Baffin Island melt inclusions are characterized by extremely low D/H ratios, from δD −97 to −218‰

[1]NASA Astrobiology Institute, Institute for Astronomy, University of Hawai'i, 2680 Woodlawn Drive, Honolulu, HI 96822-1839, USA. [2]Hawai'i Institute of Geophysics and Planetology, Pacific Ocean Science and Technology (POST) Building, University of Hawai'i, 1680 East-West Road, Honolulu, HI 96822, USA. [3]Scripps Institution of Oceanography, University California San Diego, 9500 Gilman Drive, La Jolla, CA 92093-0244, USA. [4]Department of Oceanography, University of Hawai'i, Marine Sciences Building 304, 1000 Pope Road, Honolulu, HI 96822, USA. [5]Institute for Astronomy, University of Hawai'i, 2680 Woodlawn Drive, Honolulu, HI 96822, USA.
*Present address: School of Geographical and Earth Sciences, University of Glasgow, Gregory Building, Lillybank Gardens, Glasgow G12 8QQ, UK. †Corresponding author. E-mail: lydia.hallis@glasgow.ac.uk ‡Present address: Nordic Volcanological Center, Institute of Earth Sciences, University of Iceland, Askja, Sturlugata 7, 101 Reykjavík, Iceland.

Table 1. Water content, D/H ratio (δD), and $^{18}O/^{16}O$ ratio ($\delta^{18}O$) of Baffin Island and Icelandic samples. Owing to the small size of melt inclusions in the samples, it was mostly not possible to collect hydrogen- and oxygen-isotope data from the same inclusions. Therefore, oxygen-isotope data are calculated on the basis of the average value of melt inclusions (n = 2 to 4) within the same olivine grain as that measured for D/H. Olivine oxygen data are also presented as an average (n = 2 to 6). Scanning electron microscope images showing the location of each data point on the sample surfaces are available (21).

Sample and phase	H_2O (ppm)	δD (‰)	2σ (‰)	$\delta^{18}O$ (‰)	2σ (‰)
Baffin Island picrites					
PI-16_area 4_melt inclusion 1	709	−115	38	5.18	0.25
PI-16_area 6_melt inclusion 1	926	−107	39	5.18	0.25
PI-16_area 7_melt inclusion 1	1189	−108	35	5.18	0.25
PI-16_area 8_melt inclusion 1	1039	−122	36	5.18	0.25
PI-16_area 9_melt inclusion 1	1175	−158	51	5.18	0.25
PI-16_area 9_melt inclusion 2	576	−114	40	5.18	0.25
PI-16_area 4_olivine 1	194			4.53	0.34
PI-16_area 6_olivine 1	413			4.53	0.34
PI-16_area 7_olivine 1	153			4.53	0.34
PI-16_area 8_olivine 1	200			4.53	0.34
PI-16_area 9_olivine 1	187			4.53	0.34
PI-19_area 1_melt inclusion 1	1337	−137	35	4.73	0.16
PI-19_area 1_melt inclusion 2	1465	−177	37	4.73	0.16
PI-19_area 2_melt inclusion 1	1719	−173	34	4.73	0.16
PI-19_area 2_melt inclusion 2	1964	−218	34	4.73	0.16
PI-19_area 3_melt inclusion 1	1779	−197	34	4.73	0.16
PI-19_area 6_melt inclusion 1	997	−137	32		
PI-19_area 7_melt inclusion 1	868	−97	34		
PI-19_area 8_melt inclusion 1	901	−126	32		
PI-19_area 1_olivine 1	557			4.38	0.25
PI-19_area 2_olivine 1	641			4.38	0.25
PI-19_area 2_olivine 2	712			4.38	0.25
PI-19_area 3_olivine 1	781			4.38	0.25
PI-19_area 8_olivine 1	187				
PI-19_area 8_olivine 2	190				
Icelandic picrites					
MID-1_bullet 2_melt inclusion 1	946	−88	51	4.83	0.40
MID-1_bullet 2_melt inclusion 2	964	−90	50	4.83	0.40
MID-1_bullet 3_melt inclusion 1	474	−34	53	4.83	0.40
MID-1_bullet 2_olivine 1	157			2.43	0.46
MID-1_bullet 3_olivine 1	85			2.43	0.46
NAL828_bullet 5_melt inclusion 1	600	−34	53	6.54	0.48
NAL828_bullet 5_melt inclusion 2	510	−29	53	6.54	0.48
NAL828_bullet 5_olivine 1	100			5.36	0.46
NAL 688_bullet 13_melt inclusion 1	587	−25	28	5.89	0.35
NAL 688_bullet 13_olivine 1	36			5.72	0.56

(Table 1). Melt-inclusion dehydration, where H_2O preferentially diffuses faster than HDO through encapsulating olivine, accounts for the inverse correlation between δD and water content (Fig. 1A). The longer olivine grains are resident in hot melt before eruption, the stronger the effect of dehydration (22). In addition to dehydration, melt-inclusion degassing can also raise D/H ratios and lower water contents. Melt inclusions may undergo degassing due to depressurization during eruption. We selected rapidly quenched subglacially (Iceland) and subaqueously (Baffin Island) erupted samples to mitigate the effects of degassing. However, two of the three Icelandic samples exhibit the high δD and low water contents indicative of

this process. Revealingly, sample MID-1 is known to be one of the least degassed Icelandic basalts (10) and contains melt inclusions with the lowest δD (−88 to −90‰) and highest H_2O contents [946 to 964 parts per million (ppm)] of the three Icelandic samples.

The wide spread in $\delta^{18}O$ values between samples (Table 1 and Fig. 1B) supports a heterogeneous Baffin Island and Iceland plume with respect to $\delta^{18}O$ (11, 23, 24). The Baffin Island melt inclusion $\delta^{18}O$ values (4.73 to 5.18‰) are similar to those of Baffin Island picrite matrix glasses (4.84 to 5.22‰) (25). These values are lower than typical MORB $\delta^{18}O$ [5.5 ± 0.2‰ (26)], indicating a possible correlation between low D/H, low

$^{18}O/^{16}O$, and high $^3He/^4He$ as an intrinsic property of the undegassed mantle.

Lithospheric slab dehydration during subduction and deep recycling can produce low D/H ratios in glasses from plume-related localities (17, 27). Basaltic glasses from the Hawaiian Koolau volcano contain low δD values and water contents similar to those of the Baffin Island picrites (27) (Fig. 1A). However, the Koolau mantle source is thought to contain a substantial fraction of recycled upper oceanic crust and sediment (27), and its distinct $\delta^{18}O$ (Fig. 1B) is attributed to an EM2 signature (sedimentary recycling). The Baffin Island samples do not contain any evidence of a recycled slab component (21); hence, their low δD values must be attributed to a different origin. The correlation between low D/H and high $^3He/^4He$ ratios in the Baffin Island and Iceland samples suggests that they originate from a region isolated from mixing. Thus, our data support a heterogeneous mantle, which contains deep, primitive, undegassed regions that have never been involved in subduction-related mixing or recycling (13).

Magma-ocean crystallization models (28), and Nd isotopic evidence from some of Earth's oldest rocks (29), indicate a small volume of late-solidifying dense cumulates developed during the first 30 to 75 million years of Earth history. High pressures near the base of Earth's magma ocean would cause magma to become denser than coexisting minerals; thus, crystallization would proceed from the top downward (30). Top-down crystallization would trap volatile elements in cumulates at the deepest section of the mantle. Nd-isotope data suggest that such cumulates still exist, representing a hidden incompatible-element–enriched reservoir complementary to the depleted nature of most of Earth's mantle (29, 31). The depth of this enriched reservoir explains its absence in modern-day upper-mantle melts. However, deep plume melting can transfer melt from the core-mantle boundary to the surface (32). The olivine compositions of Baffin Island picrites, as well as other samples with high $^3He/^4He$ (e.g., basalts from western Greenland and the Galapagos), suggest that these lavas originated from a peridotite source ~20% higher in Ni content than the modern depleted mantle source, apparently as a result of interaction with the Ni-rich core (5). The noble gas composition of many OIBs, including high proportions of solar Ne, suggests that these plumes sample a volatile-rich reservoir (33, 34).

The lowest measured D/H value (δD = −218‰) provides an upper limit on the D/H of early Earth if the Baffin Island picrite melt inclusions sample a deep mantle reservoir with preserved primitive volatiles. One possibility is that this strongly negative δD was added to the Earth during initial accretion, via dust grains with adsorbed H_2O inherited directly from the protosolar nebula (−870‰) (35). The temperature was high at Earth's orbital distance during the early solar system, but 1000 to 500 K would still allow adsorption of 25 to 300% of Earth's ocean water onto fractal grains during Earth's accretion (36). Solar wind hydrogen and additional accreting objects from the outer
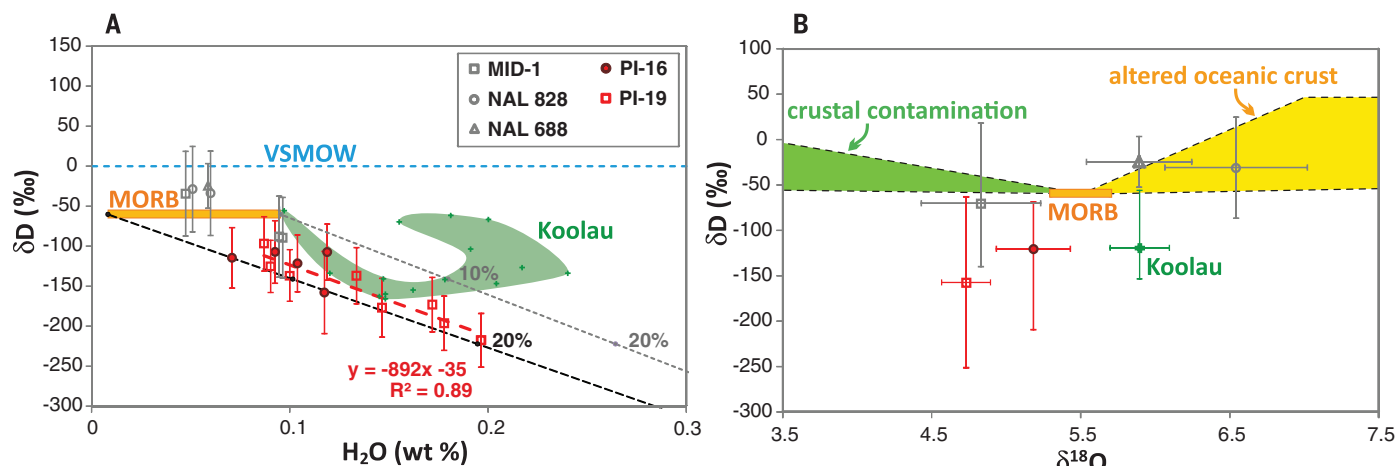
Fig. 1. Hydrogen- and oxygen-isotope ratios. The hydrogen-isotope ratios (δD) of Baffin Island and Icelandic basaltic melt inclusions versus water content (**A**) and oxygen-isotope ratios (**B**). Uncertainties are 2σ, except for (B) δD, where error bars represent the full range of the data set. The δD versus H₂O (A) data trendline gradient for sample PI-19 is shown by the red dashed line. Mixing lines between a protosolar-like deep mantle source [δD = −870‰, H₂O = 0.94 wt %] (*35*) and MORB (*19, 37*) are shown by the black and gray dashed lines, which assume minimum and maximum MORB source region H₂O contents of 0.008 and 0.095 wt %, respectively (*37*). Melt in- clusion data from the Hawaiian Koolau volcano, which contains the lowest δD values of the Hawaiian plume (*27*), are represented by the green crosses and envelope in (A) and green cross in (B). Average melt inclusion δD values are shown on the δD versus δ¹⁸O plot (B). The colored envelopes (B) indicate regions of crustal contamination, based on the δ¹⁸O variation of possible contaminants from the Icelandic crust (−7.5 to +1.65‰, green envelope) (*24*), and hydrothermally altered oceanic crust (+7 to +15‰, yellow envelope) (*26*). The δD variation of the envelopes is as reported for hydrothermally altered oceanic crust (−34 to 46‰) (*17, 18*).

part of the inner solar system may also have mixed into the accreting planet (*34*). Experimentally based atmospheric chemical models support proto- solar nebula adsorption, as they suggest an ini- tial δD between −500 and −889‰ for Earth (*2*).

The δD versus H₂O [weight percent (wt %)] correlation for Baffin Island sample PI-19 (Fig. 1A) suggests that a deep mantle source with a protosolar δD value of −870‰ would have a wa- ter content of 0.94 wt %. This value is higher than that calculated for typical bridgmanite (<220 ppm H₂O) (*37*), although post-bridgmanite can con- tain more hydrogen (*38*). In addition, isotopic ra- tios show that plume material is not typical of ambient mantle (*4–7*), and primary Hawaiian mag- mas have been shown to contain 0.36 to 0.6 wt % water (*27*). A 20/80% mixture of a protosolar-like deep mantle source (δD = −870‰, H₂O = 0.94 wt %) (*35*) and MORB (*19, 37*) reproduces the lowest measured Baffin Island δD values. This proportion is consistent with mantle Xe-isotope anomalies, also estimated to reflect admixture with about 20% of a solar Xe component (*33*).

The similarity between the bulk chemical com- position of Earth and carbonaceous chondrites indicates that Earth accreted from building blocks similar to these meteorites (*39*). An initial Earth δD value more negative than −218‰ is at the very lower end of the δD range for bulk-rock CM and CI chondrites (+338 to −227‰) (*40*), whereas other carbonaceous chondrite groups have more positive bulk-rock δD (−48 to +763‰) (*40*). However, the δD range for water in CI and CM chondrites is low (−383 to −587‰) (*40*), hinting that their parent bodies may have gained water via protosolar neb- ula adsorption. Recent reports of Earth-like δD in the martian interior (*41*) also suggest protosolar nebula adsorption as a source for martian water. Therefore, the adsorption mechanism could pro-

vide an important source of water in inner solar system terrestrial bodies.

REFERENCES AND NOTES

1. O. Abramov, S. J. Mojzsis, *Nature* **459**, 419–422 (2009).
2. H. Genda, M. Ikoma, *Icarus* **194**, 42–52 (2008).
3. A. W. Hofmann, *Nature* **385**, 219–229 (1997).
4. C. Herzberg *et al.*, *Nature* **493**, 393–397 (2013).
5. H. M. Gonnermann, S. Mukhopadhyay, *Nature* **459**, 560–563 (2009).
6. F. M. Stuart, S. Lass-Evans, J. G. Fitton, R. M. Ellam, *Nature* **424**, 57–59 (2003).
7. N. A. Starkey *et al.*, *Earth Planet. Sci. Lett.* **277**, 91–100 (2009).
8. J. Geiss *et al.*, *Space Sci. Rev.* **110**, 307–335 (2004).
9. D. R. Hilton, K. Grönvold, C. G. Macpherson, P. R. Castillo, *Earth Planet. Sci. Lett.* **173**, 53–60 (1999).
10. E. Füri *et al.*, *Geochim. Cosmochim. Acta* **74**, 3307–3332 (2010).
11. C. G. Macpherson, D. R. Hilton, J. M. D. Day, D. Lowry, K. Grönvold, *Earth Planet. Sci. Lett.* **233**, 411–427 (2005).
12. M. D. Kurz, W. J. Jenkins, S. R. Hart, *Nature* **297**, 43–47 (1982).
13. M. G. Jackson *et al.*, *Nature* **466**, 853–856 (2010).
14. I. Robillard, D. Francis, J. N. Ludden, *Contrib. Mineral. Petrol.* **112**, 230–241 (1992).
15. J. Hoefs, *Stable Isotope Geochemistry.* (Springer, Berlin, ed. 6, 2009).
16. C. Lécuyer, P. Gillet, F. Robert, *Chem. Geol.* **145**, 249–261 (1998).
17. A. M. Shaw *et al.*, *Nat. Geosci.* **5**, 224–228 (2012).
18. Q.-K. Xia *et al.*, *Geophys. Res. Lett.* **29**, 4-1-4-4 (2008).
19. M. Clog, C. Aubaud, P. Cartigny, L. Dosso, *Earth Planet. Sci. Lett.* **381**, 156–165 (2013).
20. D. Francis, *Contrib. Mineral. Petrol.* **89**, 144–154 (1985).
21. Materials and methods are available as supplementary materials on *Science* Online.
22. G. A. Gaetani, J. A. O'Leary, N. Shimizu, C. E. Bucholz, M. Newville, *Geology* **40**, 915–918 (2012).
23. A. A. Gurenko, M. Chaussidon, *Earth Planet. Sci. Lett.* **205**, 63–79 (2002).
24. M. E. Hartley, T. Thordarson, J. G. Fitton, EIMF, *Geochim. Cosmochim. Acta* **123**, 55–73 (2013).
25. A. J. R. Kent *et al.*, *Geochem. Geophys. Geosyst.* **5**, Q11015 (2004).
26. J. M. Eiler, *Rev. Mineral. Geochem.* **43**, 319–364 (2001).
27. E. Hauri, *Chem. Geol.* **183**, 115–141 (2001).
28. L. T. Elkins-Tanton, *Earth Planet. Sci. Lett.* **271**, 181–191 (2008).
29. M. Boyet, R. W. Carlson, *Science* **309**, 576–581 (2005).
30. L. T. Elkins-Tanton, *Astrophys. Space Sci.* **332**, 359–364 (2011).
31. S. Labrosse, J. W. Hernlund, N. Coltice, *Nature* **450**, 866–869 (2007).
32. D. V. Helmberger, L. Wen, X. Ding, *Nature* **396**, 251–255 (1998).
33. G. Holland, C. J. Ballentine, *Nature* **441**, 186–191 (2006).
34. M. Trieloff, J. Kunz, D. A. Clague, D. Harrison, C. J. Allègre, *Science* **288**, 1036–1038 (2000).
35. K. D. McKeegan, L. A. Leshin, *Rev. Mineral. Geochem.* **43**, 279–318 (2001).
36. M. J. Drake, *Meteorit. Planet. Sci.* **40**, 519–527 (2005).
37. W. R. Panero, J. S. Pigott, D. M. Reaman, J. E. Kabbes, Z. Liu, *J. Geophys. Res. Solid Earth* **120**, 894–908 (2015).
38. S. Akber-Knutson, G. Steinle-Neumann, P. D. Asimow, *Geophys. Res. Lett.* **32**, L14303 (2005).
39. B. Marty, *Earth Planet. Sci. Lett.* **313-314**, 56–66 (2012).
40. C. M. Alexander *et al.*, *Science* **337**, 721–723 (2012).
41. L. J. Hallis, G. J. Taylor, K. Nagashima, G. R. Huss, *Earth Planet. Sci. Lett.* **359-360**, 84–92 (2012).

Evidence for primordial water in Earth's deep mantle

Lydia J. Hallis *et al.*
Science **350**, 795 (2015);
DOI: 10.1126/science.aac4834